FY21-22 NM WRRI STUDENT WATER RESEARCH FINAL REPORT

1. STUDENT RESEARCHER: Saman Mostafazadeh-Fard: PhD Student in Civil Engineering (Minor in Computer Science), Department of Civil Engineering, New Mexico State University

2. FACULTY ADVISOR: Zohrab Samani: Professor, Department of Civil Engineering, New Mexico State University

3. PROJECT TITLE: Sediment Transport Management in New Mexico's Water Systems Using CFD Platform Flow 3-D Code

4. RELATED PUBLICATIONS:

1. Mostafazadeh-Fard S, Samani Z, Suazo K (In Review) Hydrodynamic and Sediment Transport Analysis of CFD Designed Smart Ditch. ASCE Journal of Irrigation Engineering.

2. Mostafazadeh-Fard S, Samani Z (In Review) Dissipating Culvert End Design for Erosion Control Using CFD Platform FLOW-3D Code. ASCE Journal of Irrigation and Drainage.

Abstract:

Ditch liners are used to prevent soil erosion and reduce seepage losses in water systems such as ditch liners across New Mexico. This research introduced an approach to validate a computational fluid dynamics (CFD) platform FLOW-3D code (Flow Science, Inc., Santa Fe, N.M.) and its use to design a flow regulating corrugated ditch liner system (Smart Ditch (SM)). Hydrodynamic and sediment transport analysis were performed on the proposed liner flow using CFD platform FLOW-3D code. The code's hydrodynamic and scour and sediment transport models were calibrated and validated using lab data with an accuracy of 94 % and 95%, respectively. The code was then used to measure hydrodynamic parameters of sublayer turbulent intensity, kinetic energy, dissipation and packed sediment mass normalized with respect to sublayer flow velocity. Sublayer turbulent intensity, kinetic energy, and dissipation in the SM flow was significantly higher than CR flow. An alternative corrugated liner was also designed and sediment transport was measured and compared to SM and CR flows. Normalized packed sediment mass with respect to average sublayer flow velocity was 27.8 % lower in alternative flow compared to SM flow. CFD platform FLOW-3D code could effectively be used to design corrugated ditch liner systems and perform hydrodynamic and sediment transport analysis under various corrugation designs by water agencies across the states including Elephant Butte Water District and International Boundary and Water Commission.

Keywords: CFD, hydrodynamic, sediment transport, ditch, liner design.

INTRODUCTION

Ditch liners are installed in irrigation and drainage ditches across New Mexico to prevent soil erosion, reduce seepage losses and improve their life-span. In addition, in the recent years, ditch liner systems with corrugated designs have proven to help regulate the flow of water from flat to steep grades so that the drainage and flow patterns designed are maintained. Furthermore, assessment of hydrodynamic and sediment transport parameters is among the most important elements in the design of liner systems.

Erosion, transport and deposition of sediments in ditch flows across New Mexico represents a significant impact on their operations (Hlavcova et al., 2018). Sedimentation occurs as flow velocity and turbulence levels are reduced, and can be escalated if velocity and turbulence are further reduced. As a result, dredging operations are performed to remove the deposited sediments (Bashan et al. 2013; Olsen and Hillebrand 2018). In the US, it is estimated that more than 300 million cubic meters of sediment is removed through dredging by the US Army Corp of Engineers at a cost of $8 to $12 per cubic meter annually to maintain navigation in more than 19,200 kilometers of waterways (Brandon and Price 2007). Furthermore, dredging operations are known to be time consuming (Bashan et al. 2013; Olsen and Hillebran 2018). In addition, transportation and use of dredging equipment can be risky in environmentally sensitive and uneven areas (Bashan et al. 2013; Vogt and Hartman 2018). The deposition of sediments can also have negative environmental impacts including, the loss of sensitive aquatic animals, soil erosion, loss of wetlands, and nutrient imbalance (Bashan et al. 2013; Stauber et al. 2016; Olsen and Hillebrand 2018). Therefore, there is need for an efficient and effective methodology that enables sediment transport analysis in design of ditch liner systems across New Mexico by water agencies including Elephant Butte Water District and International Boundary and Water Commission.

Additionally, the effect of hydrodynamic parameters including turbulent intensity, kinetic energy, and dissipation on the motion, suspension, entrainment, and transport of sediments has drawn significant attention in the recent years (Keshavarzy and Ball, 1997; Butler et al. 2003; Sumer et al. 2003; Tinoco and Coco 2018).

Previous researchers have shown a strong correlation between sediment particle motion, suspension, entrainment, and transport, with near-bed region (sublayer) turbulent intensity, kinetic energy, dissipation, and velocity variations (Nelson et al. 1995; Keshavarzy and Ball, 1997; Sumer et al. 2003; Tinoco and Coco 2018).

According to these studies, the settling velocity of sediment particles is suppressed or enhanced depending on relative turbulent intensity in the sublayer (Kawanisi and Shiozaki 2008). However, these studies have mostly focused on turbulent intensity that is naturally generated in the flow sublayer as a result of naturally rough bed (e.g., sand, vegetation) and flow interaction (Tachie et al. 2004; Tinoco and Coco 2018). Furthermore, Khosronejad et al. (2020) used computational fluid dynamics (CFD) to show the impact of turbulent intensity on the 3D turbulent flow field and sediment transport of large-scale rivers.

Furthermore, computational fluid dynamics (CFD) uses numerical analysis and data structures to solve fluid flow problems. Additionally, with advances that have been made on CFD, its applications combined with machine learning and artificial intelligence methods have been proven to be an accurate and efficient replacement for expensive and time-consuming in-field and experimental modeling of flows in hydraulic structures such as ditches (Chatila and Tabbara 2004; Zhenwei et al. 2012). In addition, the CFD platform FLOW-3D code is a software package that has been used in flow and sediment transport modeling due to its high performance and accuracy (Kim 2007; Montagna et al. 2011; Kim et al. 2012; Olsen and Hillebrand 2018). To date, this CFD code has not been validated for the purpose of ditch liner system design and performing hydrodynamic and sediment transport analysis on their flows.

The goal of this research was to validate the CFD platform FLOW-3D code for the purpose of corrugated liner design, and performing associated hydrodynamic and sediment transport analysis on its flow.

Accordingly, a comprehensive approach was introduced to validate the CFD platform FLOW-3D code hydrodynamic model with the use of Manning number as validation metric and its scour and sediment transport model with the use of sediment mass as validation metric. Additionally, hydrodynamic parameters of sublayer turbulent intensity, kinetic energy, dissipation and with two different sediment species (silt and sand) under smooth (CR) representing unlined ditch and modified geometric (SM) liner designs were measured and compared. This paper also proposes an new corrugated liner design (alternative) using Flow 3-D code and compares packed sediment mass reduction compared in CR, SM and alternative flows.

METHODS

GEOMETRY, MESH AND MODEL PARAMETERS

Two simulations were developed using CFD platform FLOW-3D code: 1) control ditch with smooth liner (CR); and 2) ditch with modified corrugated liner geometric design (SM).

For production of the CR and SM liner geometric models, a three-dimensional model for each geometric model was created (scale of 1:1) in AutoCAD 3D environment. The CR and SM liner geometric models consisted of a trapezoidal ditch with a length of 6 m. The SM liner geometric model consisted of ribs with height and spacing of approximately 0.08 m. The ribs were merged into the bottom of the ditch in a zigzag format. The produced liner geometric models were then exported into the FLOW-3D domain.

After importing the liner geometric models from AutoCAD 3D environment into the FLOW-3D domain, CFD platform FLOW-3D code (Flow Science, Inc., Santa Fe, N.M.) was used to accurately simulate and analyze CR and SM flows in the corresponding ditches.

An initial research was performed to investigate the optimal model parameters and mesh resolutions to be used in the simulations. The utilized design of grid cell size was based on similar studies and minimum cell sizes recommended by American Society of Mechanical Engineers (ASME) (Celik et al. 2008). A mesh block with approximately 250000 active cells was found to provide adequate aspect ratios, simulation time, computational efforts and accuracy through mesh sensitivity analysis and was used to mesh the entire computational domain (Figure 1). An additional nested mesh block with 15000 active cells was utilized to mesh the sublayer and capture the highly complex recirculating flow with grooves in this region (Figure 1). Due to the relative simplicity of the modeled geometry, structured rectangular meshes were selected and used in the simulations (Keyes et al. 2000; Bayon et al. 2016). This was done because previous studies have shown that use of structured meshes provide better accuracy (Hirsch 1988; Biswas and Strawn 1998). Their algorithms are also known to be more simple and efficient (Bayon et al. 2016).

NUMERICAL MODEL AND HYDRODYNAMIC PARAMETERS

For sediment transport modeling, two phase sediment transport modeling was implemented using CFD platform FLOW-3D code (Flow Science, Inc., Santa Fe, N.M.). Hydrodynamic analysis was performed based on two-phase area/volume obstacle representation (Favor) methodology available in CFD platform FLOW-3D code (Hirt and Nichols, 1981; Hirt 2011).

The Favor methodology was used to capture the complex liner geometric designs and to solve the highly complex recirculating flow with grooves in the vicinity of the walls (FLOW-3D 2016; Daraghi 2010). In this approach, structured rectangular grids whose elements are assigned to fractional areas and volumes are utilized for modeling (FLOW-3D 2016; Hirt 2011). For turbulence modeling, standard k-ε was implemented in the simulations (Versteeg et al. 2007; Daraghi 2010).

FLOW-3D CFD simulations provided data sets on turbulent intensity, turbulent kinetic energy and turbulent dissipations for each flow. These data sets were generated based on the following formulas for each parameter :

Turbulent intensity (percentage) parameter (I) used in this study can be defined using the following equation:

$$I = \frac{u'}{\tilde{u}} \times 100 \ (1)$$

Where u' is the mean velocity of the fluid in the sublayer region and $\tilde{u}$ is the fluctuation of the streamwise velocity component.

Turbulence dissipation, ε, is the rate at which turbulence kinetic energy (*k*) is converted into thermal internal energy. *k* can be defined using the following equation:

$$k = \frac{3}{2} u''^2 \ (2)$$

Where u'' is the flow turbulent fluctuation.

Newly added scour and sediment transport model to FLOW-3D (Version 11.2) was used for sediment transport modeling (FLOW-3D 2016; Chen 2006). In this model, sediment particle characteristics are considered to be uniform. The FLOW-3D hydrodynamic solver is completely coupled with the embedded scour and sediment transport model that simulates suspended and bed load sediment transport, erosion and entrainment for non-cohesive soils (Hirt 2011; Wei et al. 2014). FLOW-3D*'s* hydrodynamic model solves the complete unsteady non-hydrostatic Reynolds-averaged Navier-Stokes equations that describe the physics of the flow.

Suspended load and bed load is evaluated separately for sedimentary computing section. Suspended sediment load is acquired by solving the transient convection-diffusion equation (equation 3) (Pourshahbaz and Abbasi 2017).

$$\frac{\partial c}{\partial t} + U_i \frac{\partial c}{\partial c_i} + W \frac{\partial c}{\partial z} = \frac{\partial}{\partial x_i}\left(\Gamma \frac{\partial c}{\partial x_i}\right) \quad (3)$$

Where U=Reynolds-average water velocity, W= fall velocity of sediment, x=general space dimension, z= dimension in the vertical direction, Γ= diffusion coefficient. The diffusion coefficient is equal to flow eddy viscosity which is calculated by The $k - \varepsilon$ model. This equation explains sediment transport which includes the effect of the turbulence on deceleration (Pourshahbaz and Abbasi 2017).

For sediment transport modeling in FLOW-3D in the near surface loads, Van Rijn equation model was used in this study. For surface cells in this model, sediment concentration and bed load are calculated by (Van Rijn, 1987) equation respectively, which are presented in equations 3 and 4:

$$C_{bed} = 0.015 * \frac{d^{0.3}\left(\frac{\tau-\tau_c}{\tau_c}\right)^{1.5}}{g\left(\frac{\rho_s-\rho_w}{\rho_w v^2}\right)^{0.1}} \quad (4)$$

In which d= diameter of sediment particle, τ= bed shear stress, τ_c =critical shear stress for sediment particle motion according to Shields diagram, ρ_s is the sediment particle density, and ρ_w= water density, v = Kinematic viscosity of water and g= gravitational acceleration.

FLOW-3D scour and sediment transport model also utilizes the bed-load sediment transport rate formula that is dependent on drag force and momentum exchange between fluid and sediment particles to model the bed-load sediment. This type of formula takes the drag force as the main factor in measuring the bed-load sediment transport rate. In this model, the sediment transport rate increases with the drag force and the drag law controls the coupling between particle and fluid. Entrainment in this model takes place by the process in which turbulent eddies remove the sediment grains from the top of the packed bed or the ditch bed and transition to the suspended state.

To study the sediment transport in simulated flows, packed sediment mass was measured and compared between flows. FLOW-3D scour and sediment transport model enables extraction packed sediment mass versus time. Table 1 summarizes the model setup selected through validation and calibration process for producing the simulations.

Table 1. Summary of CFD model setup.

Mesh	Structured Favor
Turbulence model	Standard k-ε
Solid contours	No slip, smooth surface, high Re wall function
Advection scheme	Explicit 2nd order limited (Van Leer, 1977)
Diffusion scheme	Explicit 2nd order
Courant number limit	0.75
Multiphase treatment	Favor

Free surface tracking	Donor-acceptor method (Hirt and Nichols, 1981)
Aeration	Eulerian approach
Aspect ratio	1.02

BOUNDARY CONDITIONS

The boundary of the sublayer viscous flow region attached to solid boundaries (side-walls and bed of the ditch) was set to smooth wall. The upper boundary condition was set to symmetry. To produce real-world conditions, flows were simulated as free surface flows (surface boundary condition adjusted to symmetry). The pressure on the surface of the entire flow was set to atmospheric pressure to represent free-surface effects (i.e., zero gradient).

In this scenario, null von Neumann conditions were imposed to every variable except for pressure, which was set to atmospheric pressure (i.e. zero) (Cheng and Cheng 2005). The condition of lower boundary (downstream) was set to outflow, that allowed the flow to leave the domain freely.

The condition of upper boundary of the ditch was set to constant depth and flow rate (Q = 0.02 m^3/sec; velocity = 0.3 m/sec) in flows. To achieve this flow rate, the velocity at the upstream boundary was set uniformly parallel to the ditch bottom and center line. This inflow condition was selected since 0.3 m/sec is close to critical velocity that would keep sediments in suspended state (Stoeber 2005).

Figure 1 visualizes the boundary conditions of the CFD model used for CR and SM flows.

The boundary conditions and inflow rates were the same for both CR and SM flows, ensuring that the any change in turbulent intensities, turbulent dissipation, turbulent kinetic energy or packed sediment mass in the corresponding flows is caused by the modification of the liner geometric design. To allow the flow to reach its fully developed form at each simulation, the finish time was set to 40 seconds (t = 40 s) for CR and SM flows. The height of boundary walls (including freeboard) was limited to 0.4 m for CR and SM flows (Figure 1). Figure 2 visualizes instant representation of the SM flows in FLOW-3D environment at various time points (t = 5, 10 and 20 sec).

(a)

(b)

(c)

Fig. 2. Instant representation of the SM flow in FLOW-3D environment at t=5 sec (a); t=10 sec (b) and t=20 sec (c).

MESH SENSITIVITY ANALYSIS

Mesh sensitivity was analyzed using three grid sizes of 0.025, 0.027, 0.03 m for CR flow. Manning number for each simulation was extracted and compared. Characteristics of the mesh systems used in the mesh sensitivity analysis can be seen in Table 2.

Table 2. Mesh characteristics used for sensitivity analysis for CR flow.

Mesh Type	Number of Cells in Mesh Bock	Minimum Cell Size (m)	Measured Manning Number
M1	200000	0.03	0.012
M2	250000	0.027	0.011
M3	300000	0.025	0.011

To minimize simulation time, computational efforts and maximize accuracy, it was deemed that M2 with 250000 active cells and minimum cell size of 0.027 was appropriate for the simulations (Table 2).

MODEL VALIDATION

In order to validate the CFD simulation outcome, a physical SM liner design with similar dimensions was constructed and installed at the Hydraulics Laboratory of the New Mexico State University (Figure 3). The system consisted of corrugated polyethylene liner, a recirculation tank and a water pump that was employed to provide the desired flow rate. A 90-degree PVC fitting was used to introduce water to the constructed ditch to ensure a smooth transition from pressurized to free surface flow. The CFD platform FLOW-3D code was validate and calibrated using experimental flow data. A comprehensive approach was used to validate the used hydrodynamic model of CFD platform FLOW-3D code through comparison of Manning numbers obtained from CFD simulations and experimental flows. Compared with the experimental flow data, the Manning number predicted by CFD simulation differed only by 6% and produced an approximately 94 % accuracy. Furthermore, the Manning number was measured at 0.05 for SM flow compared to 0.01 for CR flow. The higher Manning number in SM flow compared to CR is due to higher roughness of ditch under the SM liner geometric design compared to CR.

To validate and calibrate the scour and sediment model of FLOW-3D code, sediment mass was used as validation metric. For this purpose, 0.5 kg of dry sediment (90% sand; 10% silt) was placed on the entry of the ditch bottom, flow ($Q = 0.02\ m^3/sec$; velocity = 0.3 m/sec) was allowed into the ditch and the remaining deposited sediment mass after t=40 sec was collected and dried in oven and the dry mass was measured at 0.43 kg. The experimental flow was also simulated using FLOW-3D code and associated calibrated parameters and remaining sediment mass in the flow domain after t=40 sec was measured at 0.41 kg.

The validation metric predicted by CFD differed only by 5 % and produced an approximately 95 % accuracy.

Fig. 3. Flow in constructed ditch with SM liner design.

DATA COLLECTION AND ANALYSIS

Data sets on studied parameters including turbulent intensity, kinetic energy, dissipation were direct outputs of the CFD simulations. After reaching steady state condition in the flows (all flows were in a fully turbulent regime) data sets on turbulent intensity, kinetic energy, and dissipation from CR and SM flows were generated, visualized and compared.

To extract sublayer turbulent intensity, kinetic energy and dissipation, data collection points were selected with a clearance of about one-fifth (0.2) of the nominal flow depth (D (z-axis depth)) from ditch bed along the center-line of the flow. This depth, (0.2 of the nominal depth) was selected based on similar previous studies which have shown that the velocity gradient at this depth in a flow is mainly generated by the shear stress of the viscous sublayer (Wang et al. 2018). Sublayer turbulent intensity, kinetic energy and dissipation were measured using these data collection points for CR and SM flows (Tachie et al. 2004).

SEDIMENT SPECIE CHARACTERISTICS

Two sediment species (silt and sand) were selected and used in the simulations. The characteristics of the sediment species and scour and sediment parameters that were selected through validation and calibration process are shown in Table 3.

Table 3. Characteristics of the sediment species and scour and sediment parameters .

Characteristic	Sediment Specie 1 (Silt)	Sediment Specie 2 (Sand)
Type	Non-cohesive	Non-cohesive
Diameter (mm)	0.3	0.5
Density (kg/)	1120	1500
Angle of repose (Degrees)	32	32
Maximum Packing Fraction	0.64	0.64
Bed roughness / d50 ratio	5	5
Bed load transport rate equation	Van Rijn (1987)	Van Rijn (1987)

RESULTS AND DISCUSSIONS

SUBLAYER TURBULENT INTENSITY

Figure 4 visualizes sublayer turbulent intensity in CR and SM flows. Sublayer turbulent intensity reached 30 % in SM flow at x = 6 m (near outflow) and reached approximately 9 % in CR flow at x = 6 m. Sublayer turbulent intensity demonstrated an ascending pattern from x = 1 m to x = 6 m in SM flow. This profile has emerged as mainly flat from x = 0 to 5 m in CR flow. Sublayer turbulent intensity was significantly higher in SM flow compared to control flow.

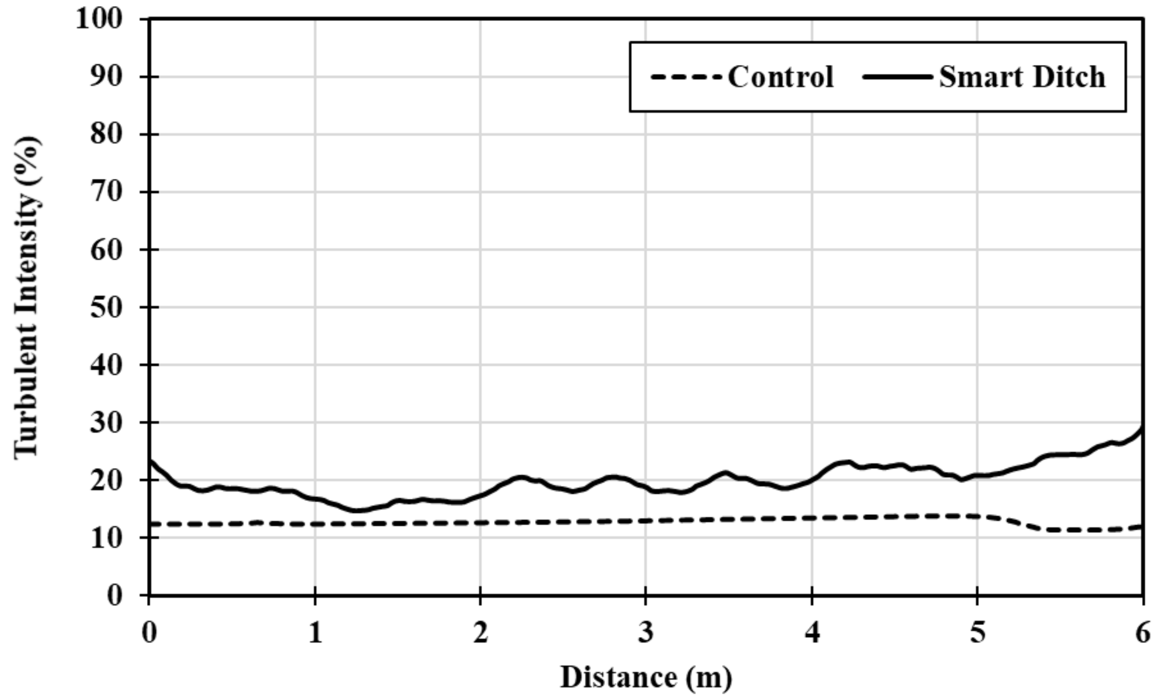

Fig. 4. Sublayer turbulent intensity in CR and SM flows.

According to Figure 4, sublayer turbulent intensity has increased significantly in SM flow compared to the CR flow. This conforms to previous reports that modification of liner geometric design in a flow can result in major increase the turbulent intensity (Tachie et al. 2004).

This increase in turbulent intensity produces stochastic shear stress fluctuations in the sublayer (Keshavarzy and Ball, 1997). These fluctuations promote the sweep and ejection events can affect sediment suspension and motion, especially when mean shear stress in sublayer is closer to threshold conditions (Sumer et al. 2003; Tachie et al. 2004; Keshavarzy and Ball, 1997).

SUBLAYER TURBULENT DISSIPATION

Figure 5 visualizes sublayer turbulent dissipation in CR and SM flows. Sublayer turbulent dissipation reached 0.025 $m^2\ s^{-3}$ in SM flow at approximately x = 6 m (near outflow) and reached 0.08 $m^2\ s^{-3}$ in CR flow at approximately x = 5 m.

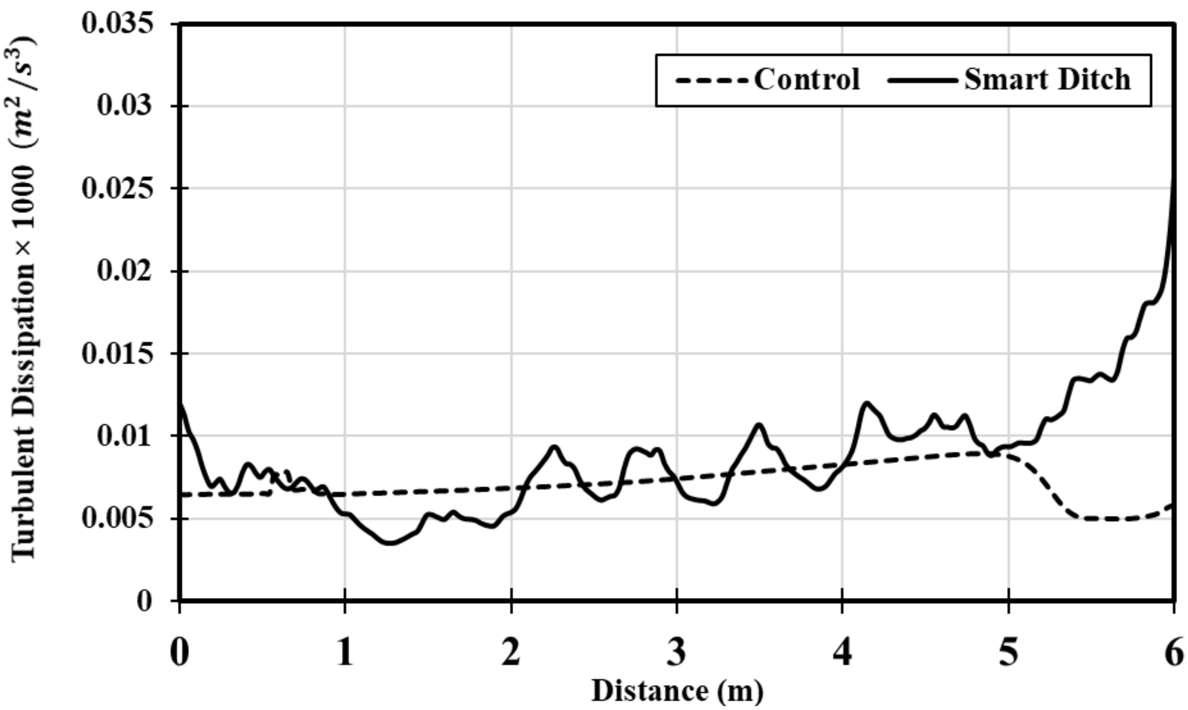

Fig. 5. Sublayer turbulent dissipation in CR and SM flows.

According to Figures 4 and 5 and similar to sublayer turbulent intensity, sublayer turbulent dissipation has increased significantly in SM flow compared to CR flow. This increase in turbulent dissipation in the sublayer is associated with sweeping events which can affect sediment suspension and motion in the sublayer region (Zaripov et al. 2020). This profile has demonstrated and ascending pattern from x = 0 to x = 5 m in CR flow and a descending pattern from x = 5 m towards outflow in CR flow.

SUBLAYER TURBULENT ENERGY

Figure 6 visualizes sublayer turbulent energy profiles in CR and SM flows. Sublayer turbulent energy reached 0.012 $m^2\ s^{-2}$ in SM flow at approximately x = 6 m (near outflow) and reached 0.0045 $m^2\ s^{-2}$ in CR flow at approximately x = 6 m.

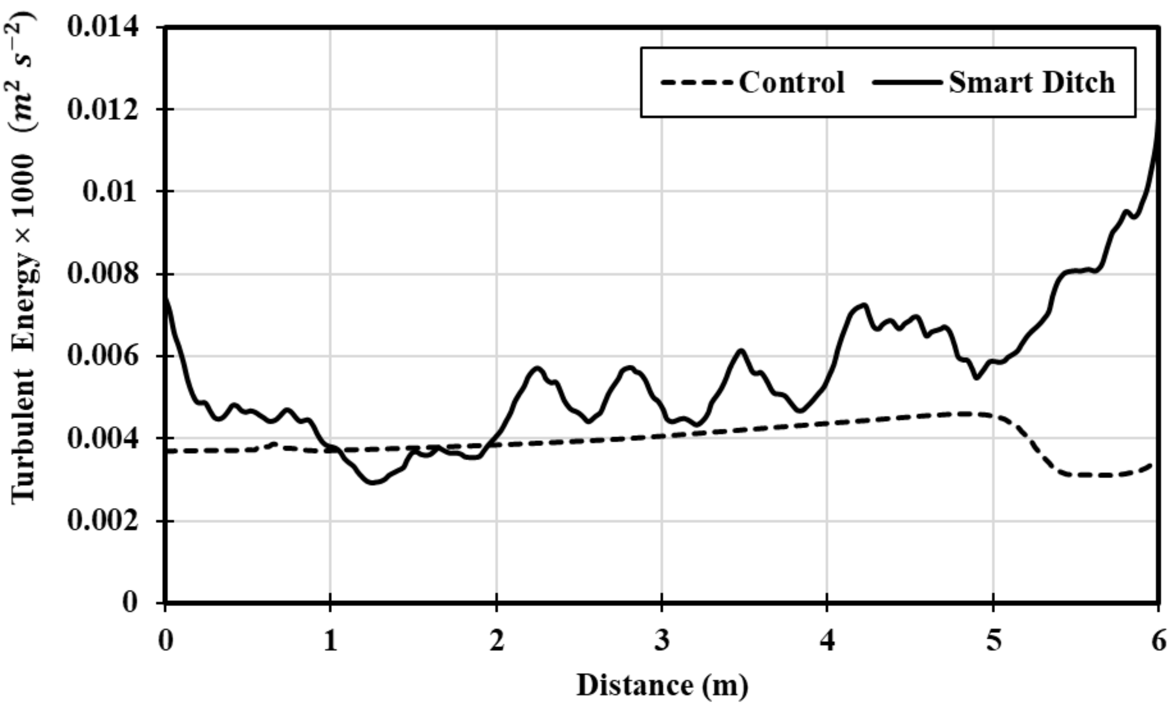

Fig. 6. Sublayer turbulent energy in CR and SM flows.

According to Figures 4 through 6, and similar to turbulent intensity and dissipation, sublayer turbulent energy has increased significantly in SM flow compared to CR flow. This profile has emerged as ascending from x = 0 to x = 5 m in CR flow while a local maximums have emerged along SM flow. Turbulent energy has demonstrated an descending pattern from x = 5 m to x = 6 m in CR flow.

The increase in sublayer turbulent energy in SM flow compared to control can be linked to interaction of sublayer with the rough bed (Tachie et al. 2004). This higher rates in sublayer turbulent energy can increase the Reynolds shear stresses (Tachie et al. 2004). The Reynolds shear stresses can be divided into two parts; one as a form of a drag and the other one that acts directly on the surface as skin friction which governs the sediment particle suspension rate (Barenblatt and Golitsyn1974; Sumer et al. 2003).

SEDIMENT TRANSPORT IN LINER FLOW

Packed sediment mass reduction in CR, SM and alternative liner flows (Figure 7) was investigated. The alternative liner model consisted of a trapezoidal ditch with a length of 6 m. It consisted of ribs with height of 0.02 m and spacing of approximately 0.1 m.

For this purpose, under similar inflow conditions (Q = 0.02 m^3/sec; velocity = 0.3 m/sec), 0.5 kg of packed sediment (50% silt and 50% sand) was placed 1.5 m away from the inflow on each simulated liner bed. Packed sediment mass in the entire flow domain at each time step (Δt = 1 sec) for 40 seconds was measured for each simulation and compared. This time frame was selected to allow the flows to reach their steady state. The average flow velocity in sublayer in in CR, SM and alternative liner flows was measured at 0.79, 0.71 and 0.73 m/sec. The packed sediment mass normalized with respect to sublayer flow velocity reduced to 0.09, 0.18, and 0.13 kg.m/sec in CR, SM and alternative liner flows respectively. Normalized packed sediment mass was 27.8 % lower in alternative flow compared to SM flow at t = 40 sec.

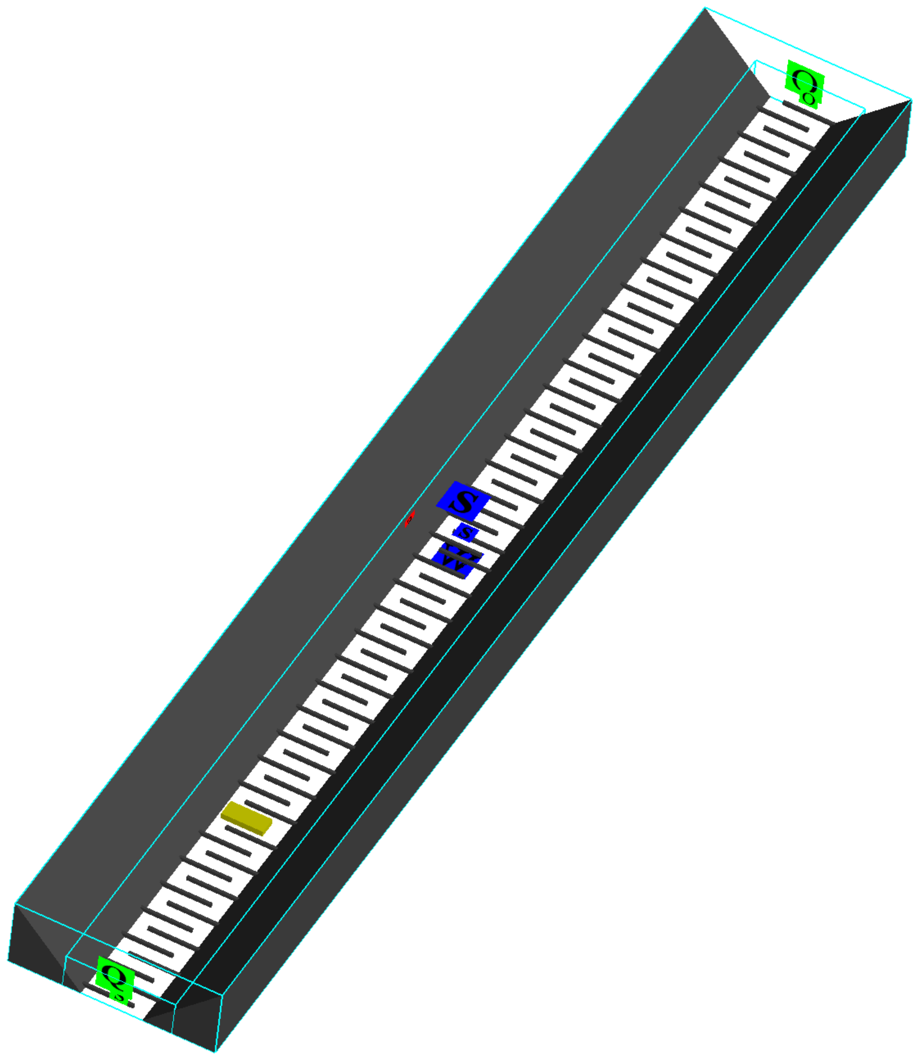

Figure 7. Proposed alternative liner design and packed sediment mass shown in yellow (t=0 sec).

Figure 8. Total sediment mass versus time in control, smart ditch and alternative liner.

Reduction in normalized packed sediment mass in alternative flow can be correlated to increase in sublayer turbulent intensity and sediment particle motion, suspension, entrainment, and transport (Yang et al. 2016; Tang et al. 2019). Since the ribs present in the bottom of the alternative flow prevent packed sediments to be dragged out of flow domain, its entrainment into the flow and exit from the flow domain that result in packed sediment mass reduction can be linked to increase in sublayer turbulent intensity, energy dissipation and associated sediment suspension (Tachie et al. 2004; Tinoco and Coco 2018). These results conform to previous reports that signify sublayer turbulent intensity as the main driver of sediment motion, and suspension (Yang et al. 2016; Tinoco and Coco 2018). Using the same methodology, sediment transport under various alternative liner designs can be investigated and compared. The liner that provides maximum packed sediment mass reduction for various case specific inflow condition can be selected for use.

Selected liner design can be manufactured using polyethylene and can be used to line ditches. The proposed liner technology also provides the benefit of covering voids present in the body of ditches and reducing erosion and seepage loss. In addition, its flexibility makes installation fast and easy with minimal environmental disturbance.

CONCLUSIONS

1. CFD platform FLOW-3D code hydrodynamic model was validated for the purpose of corrugated liner design with the use of Manning number as validation metric. FLOW-3D scour and sediment transport model was also validated with the use of sediment mass as validation metric with acceptable accuracy.

2. A CFD approach for liner design, hydraulic and sediment transport analysis in waterways and ditches across New Mexico was introduced in the paper that can be used by water agencies such as Elephant Butte Water District and International Boundary and Water Commission. This approach could replace expensive and time-consuming in-field approaches.

3. Sublayer turbulent intensity, energy and dissipation increased significantly in SM flow compared to CR flow.

3. Under the proposed alternative corrugated liner design, decrease in normalized packed sediment mass was significantly higher than SM flow.

4. This methodology of analyzing sediment transport in waterways and ditches in terms of their suspended sediment mass using CFD platform FLOW-3D code can be used to improve engineering design in waterways and ditches across New Mexico by water agencies such as Elephant Butte Water District and International Boundary and Water Commission.

5. Designed liners with FLOW-3D code can be manufactured using polyethylene and can be used to line ditches. Use of proposed technology can also reduce erosion and seepage loss in ditches. In addition, its flexibility makes installation fast and easy with minimal environmental disturbance. Implementation of corrugation in liner design would also help regulate the flow of water from flat to steep grades so that the drainage and flow patterns designed are maintained.

6. The feasibility of the proposed technique should be investigated for various case specific inflow conditions and sediment species.

DECLARATIONS

COMPLIANCE WITH ETHICAL STANDARDS

The authors declare that they have no conflict of interest.

DATA AVAILABILITY STATEMENT

Some or all data, models, or code that support the findings of this study are available from the corresponding author upon reasonable request.

FUNDING STATEMENT

This work was supported by the New Mexico Water Resource Research Institute (NMWRRI) (Fund Number NMWRRI-SG-2021). The authors appreciate New Mexico Water Resource Research Institute (NMWRRI) for its support for this research.

FUTURE PLANS

After completing my PhD in Civil Engineering at New Mexico State University, I plan on continuing my career in Aecom as a government consulting firm and eventually moving to a management role in a State Water Board or Agency.

REFERENCES

Bashan Y, Moreno M, Salazar BG, Alvarez L (2013) Restoration and recovery of hurricane-damaged mangroves using the knickpoint retreat effect and tides as dredging tools. Journal of Environmental Management 116: 196-203 https://doi.org/10.1016/j.jenvman.2012.11.045

Bayon A, Valero D, García-Bartual R, Vallés-Morán FJ, Lopez-Jiminez PA (2016) Performance assessment of OpenFOAM and FLOW-3D in the numerical modeling of a low Reynolds number hydraulic jump. Environmental Modeling Software 80:322-335 https://doi.org/10.1016/j.envsoft.2016.02.018

Barenblatt GI, Golitsyn GS (1974). Local Structure of Mature Dust Storms. Journal of Atmospheric Sciences 31(7):1917-1933. DOI: https://doi.org/10.1175/1520 0469(1974)031<1917:LSOMDS>2.0.CO;2

Biswas R, Strawn RC (1998) Tetrahedral and hexahedral mesh adaption for CFD problems. Applied Numerical Math 26:135-151 https://doi.org/10.1016/S0168-9274(97)00092-5

Brandon DL, Price RA (2007) Summary of Available Guidance and Best Practices for Determining Suitability of Dredged Material for Beneficial Uses. Vicksburg, Mississippi: U.S. Army Corps of Engineers, Dredging Operations and Environmental Research Program, ERDC/EL TR-07-27: 97 Butler R, May R, Ackers J (2003) Self-cleansing sewer design based on sediment transport principles. Journal of Hydraulic Engineering ASCE 129(4): 276-282 https://doi.org/10.1061/(ASCE)0733-9429(2003)129:4(276)

Celik IB, Ghia U, Roache PJ (2008) Procedure for estimation and reporting of uncertainty due to discretization in CFD applications. American Society of Mechanical Engineers (ASME) Journal of Fluids Engineering 130 (7): 1-4 https://doi.org/10.1115/1.2960953

Chatila J, Tabbara M (2004) Computational modeling of flow over an ogee spillway. Computers and Structures 82:1805–1812 https://doi.org/10.1016/j.compstruc.2004.04.007

Chen B (2006) The numerical simulation of local scour in front of a vertical-wall breakwater. Journal of Hydrodynamics 18(3): 134-138

Cheng AHD, Cheng DT (2005) Heritage and early history of the boundary element method. Engineering Analysis with Boundary Elements 29(3): 268 https://doi.org/10.1016/j.enganabound.2004.12.001

Dargahi B (2010) Flow characteristics of bottom outlets with moving gates. Journal of Hydraulic Research 48(4), 476–482.

Zaripov D, Li R, Saushin I (2020) Extreme events of turbulent kinetic energy production and dissipation in turbulent channel flow: particle image velocimetry measurements. Journal of Turbulence 21(1), 39-51, DOI: 10.1080/14685248.2020.1727914

Dunn C, Lopez F, Garcia M (1996) Mean flow and turbulence in a laboratory channel with simulated vegetation. Dissertation, University of Illinois at Urbana-Champaign, Urbana, IL.

Flow Science, Inc (2016) FLOW-3D Version 11.2 User Manual; Flow Science, Inc.: Los Alamos, NM, USA.

Gessler D (2005) CFD modeling of spillway performance. The Impacts of Global Climate Change 1:1-10 doi:10.1061/40792(173)398 https://doi.org/10.1061/40792(173)398.

Griffith RA, Rutherford JH, Alavi A, Moore D, Groeneveld J (2007) Stability review of the Wanapum spillwayusing CFD analysis. Canadian Dam Association Bulletin 1: 16–26.

Karim F (1999) Bed form geometry in sand-bed flows. Journal of Hydraulic Engineering 125(12): 1253-1261 doi:10.1061/(ASCE)0733-9429

Hirsch C (1988) Numerical computation of internal and external flows. Wiley and Sons, New York.

Hirt CW, Nichols BD (1981) Volume of fluid (VOF) method for the dynamics of free boundaries. Journal of Computational Physics 39:201-205 https://doi.org/10.1016/0021-9991(81)90145-5

Hirt CW (2011) CFD-101: The Basics of Computational Fluid Dynamics Modeling, FLOW-3D Manual, Flow Science Press, Flow Science, Inc., Santa Fe.

Keyes D, Ecer A, Periaux J, Satofuka N (2000) Parallel computational fluid dynamics: towards teraflops, optimization, and novel formulations. Proceedings of the Parallel CFD99 Conference, Elsevier, New York, 2000

Kim D (2007) Numerical analysis of free flow past a sluice gate. KSCE Journal of Civil Engineering 11(2):127–132 https://doi.org/10.1007/BF02823856

Kim S, Yu K, Yoon B, Lim Y (2012) A numerical study on hydraulic characteristics in the ice Harbor-type fishway. KSCE Journal of Civil Engineering 16:265–272 https://doi.org/10.1007/s12205-012-0010-5

Kirkgoz MS, Ardichoglu M (1997) Velocity profiles of developing and developed open channel flow. Journal of Hydraulic Engineering 123(12):1099–1105 https://doi.org/10.1061/(ASCE)0733-9429(1997)123:12(1099).

Khosronejad A, Flora K and Kang (2020) Effect of inlet turbulent boundary conditions on scour predictions of coupled LES and morphodynamics in a field-scale river: Bankfull flow conditions" Journal of Hydraulic Engineering 146(4), 04020020

Kawanisi K, Shiozaki R (2008) Turbulent effcts on the settling velocity of suspended sediment. Journal of Hydraulic Engineering 134, 261–266 DOI: 10.1061/(ASCE)0733 9429(2008)134:2(261).

Keshavarzy A, Bal JE (1997) An analysis of the characteristics of rough bed turbulent shear stresses in an open channel. Stochastic Hydrology Hydraulics 11, 193–210. DOI: https://doi.org/10.1007/BF02427915

Lambkin DO, Collins MB, Paphitis D (2004) Wave period and flow asymmetry effects on the transition to turbulence in relation to sediment dynamics. Journal of Geophysic Research 109: F03009. DOI: https://doi.org/10.1029/2003JF000074

Liu X and Garcia M H (2008) Three-dimensional numerical model with free water surface and mesh deformation for local sediment scour Journal of Waterway Port Coastal Ocean Engineering. 134: 203–17

Pourshahbaz H, Abbasi S (2017) Numerical scour modeling around parallel spur dikes in FLOW-3D. Drinking Water Engineering and Science Discussions, 1-16.

Mu Z, Zhiyan Z, Tao Z (2012) Numerical simulation of 3-D flow field of spillway based on VOF method. Procedia Engineering 28:808–812 https://doi.org/10.1016/j.proeng.2012.01.814

Montagna F, Bellotti G, DiRisio M (2011) 3D numerical modeling of landslide-generated tsunamis around a conical island. Natural Hazards 58:591-608 https://doi.org/10.1007/s11069-010-9689-0

Nelson JM, Shreve RL, McLean SL, Drake TG (1995) Role of near-bed turbulence in bed load transport and bed form mechanics. Water Resources Research 31(8): 2071–2085 https://doi.org/10.1029/95WR00976

Olsen NRB, Hillebrand G (2018) Long-time 3D CFD modeling of sedimentation with dredging in a hydropower reservoir. Journal of Soils Sediments 18: 3031–3040 https://doi.org/10.1007/s11368-018-1989-0

Stauber JL, Chariton A, Apte S (2016) Chapter 10 - Global Change, Marine Ecotoxicology, Academic Press, 273-313. ISBN 9780128033715.

Stoeber MW (2005). Minimum Velocities for the Suspension of Fine Sediment in the Green River Canal.

Shiono K, Chan TL, Spooner J, Rameshwaran P, Chandler JH (2009) The effect of floodplain roughness on flow structures, bedforms and sediment transport rates in meandering channels with overbank flows: Part II. Journal of Hydraulic Research 47(1): 20-28 https://doi.org/10.3826/jhr.2009.2944-I

Sumer BM, Chua, LHC, Cheng NS, Fredsoe J (2003) The influence of turbulence on bedload sediment transport. Journal of Hydraulic Engineering ASCE 129(8): 585-596 https://doi.org/10.1061/(ASCE)0733-9429(2003)129:8(585)

Tang C, Li Y, Acharya K (2019) Impact of intermittent turbulent bursts on sediment resuspension and internal nutrient release in Lake Taihu, China. Environmental Science and Pollutant Research 26:16519–16528 https://doi.org/10.1007/s11356-019-04847-2

Tachie MF, Bergstrom DJ, Balachandar R (2004) Roughness effects on the mixing properties in open channel turbulent boundary layers. Journal of Fluids Engineering 126(6): 1025-1032 https://doi.org/10.1115/1.1792265

Tinoco R, Coco G (2018) Turbulence as the main driver of resuspension in oscillatory flow through vegetation. Journal of Geophysical Research: Earth Surface, 123:891–904. https://doi.org/10.1002/2017JF004504

Van Leer B (1977) Towards the ultimate conservative difference scheme III. Up-stream-centered finite-difference schemes for ideal compressible flow. Journal of Computational Physics 23(3): 263-275 https://doi.org/10.1016/0021-9991(77)90094-8

Van Rijn, LC (1987). Mathematical modeling of morphological processes in the case of suspended sediment transport (pp. Communication-No). Delft: Water loopkundig Laboratorium

Versteeg HK, Malalasekera W (1995) An introduction to computational fluid dynamic: The finite volume method. John Wiley and Sons Inc, New York.

Vogt C and Hartman G (2018) Dredging practices and environmental considerations. In: Meyers R. (eds) Encyclopedia of Sustainability Science and Technology. Springer, New York, New York. https://doi.org/10.1007/978-1-4939-2493-6_438-3

Vongvisessomjai N, Tingsanchali T, Babel MS (2010) Non-deposition design criteria for sewers with part-full flow. Urban Water Journal 7(1):61-77 https://doi.org/10.1080/15730620903242824

Wang Y, Zhang H, Yang P, Wang Y (2018) Experimental Study of Overland Flow through Rigid Emergent Vegetation with Different Densities and Location Arrangements. Water 10(1) 1638 -

1640.Wei G, Brethour JM, Grünzner M, Burnham J (2014) The sedimentation scour model in FLOW-3D, Technical Note FSI-14-TN-99, Flow Science, Inc.

Yang JQ, Chung H, Nepf, HM (2016) The onset of transport in vegetated channels predicted by turbulent kinetic energy. Geophysical Research Letters 43(21):11261-11268 https://doi.org/10.1002/ 2016GL071092.

Hlavcova, K.; Kohnova, S.; Velisková, Y.; Studvova, Z.; Socuvka, V.; Ivan, P. Comparison of two concepts for assessment of sediment transport in small agricultural catchments. J. Hydrol. Hydromech. 2018, 66, 404–415.

TABLE OF ABBREVIATIONS

Abbreviation	Meaning
u'	Mean velocity of the fluid in the sublayer region
$\tilde{u}$	Fluctuation of the streamwise velocity component
u''	Flow turbulent fluctuation.
U	Reynolds-average water velocity
W	Fall velocity of sediment.
z	Dimension in the vertical direction
x	General space dimension
Γ	Diffusion coefficient
d	Diameter of sediment particle

τ_c	critical shear stress for sediment particle motion according to Shields diagram
ρ_s	Sediment particle density
ρ_w	water density
g	gravitational acceleration
ν	Kinematic viscosity of water and
τ	bed shear stress

FIGURE CAPTIONS

Fig. 1. (a) Boundary conditions of the CFD model and sediment box used for CR and SM flows. (b) SM liner geometric model. (c) cross section of simulated ditch.

Fig. 2. Instant representation of the SM flow in FLOW-3D environment.

Fig. 3. Flow in constructed ditch with SM liner design.

Fig. 4. Sublayer turbulent intensity in CR and SM flows.

Fig. 5. Sublayer turbulent dissipation in CR and SM flows.

Fig. 6. Sublayer Turbulent energy in CR and SM flows.

Fig. 7. Proposed alternative liner design and packed sediment mass shown in yellow (t=0 sec).

- **Include a paragraph on who will benefit from your research results. Include any water agency that could use your results.**

Agencies across the states including Elephant Butte Water District and International Boundary and Water Commission as well as State Water boards and government consulting firms would be able to recommend the implementation of proposed liner design technology to contractors.

- **Describe how you have spent your grant funds.**

The funding was used to support the research of this project. The funds were used to support the salary and fringe of a Graduate Research Assistantship in Summer 2021 & 2022.

- **List presentations you have made related to the project.**

N/A

- **List publications or reports, if any, that you are preparing. Thank you for attributing the funding to NM WRRI and the New Mexico State Legislature by including the account number: NMWRRI-SG-2021.**

1. Mostafazadeh-Fard S, Samani Z, Suazo K (In Review) Hydrodynamic and Sediment Transport Analysis of CFD Designed Smart Ditch. ASCE Journal of Irrigation Engineering.

2. Mostafazadeh-Fard S, Samani Z (In Review) Dissipating Culvert End Design for Erosion Control Using CFD Platform FLOW-3D Code. ASCE Journal of Pipeline Systems - Engineering and Practice.

- **List any other students or faculty members who have assisted you with your project.**

N/A

- **Provide special recognition awards or notable achievements as a result of the research, including any publicity such as newspaper articles or similar.**

N/A

- **Provide information on degree completion and future career plans. Funding for student grants comes from the New Mexico Legislature. Legislators are interested in whether recipients of these grants go on to complete academic degrees and work in a water-related field in New Mexico or elsewhere.**

After completing my PhD in Civil Engineering at New Mexico State University, I plan on continuing my career in Aecom or any other government consulting firm and eventually moving to a management role in a State Water Board or Agency.